17

Polypropylene Nanocomposite Reinforced with Rice Straw Fibril and Fibril Aggregates

Yan Wu[1], Dingguo Zhou[1], Siqun Wang[2],
Yang Zhang[1] and Zhihui Wu[1]
[1]*Nanjing Forestry University*
[2]*University of Tenneessee*
[1]*China*
[2]*USA*

1. Introduction

High thermoplastic content composites are those in which the thermoplastic component exists in a continuous matrix and the lignocellulosic component serves as reinforcing filler. The great majority of reinforced thermoplastic composites available commercially use inorganic materials as their reinforcing fillers, e.g., glass, clays, and minerals. These materials are heavy, abrasive to processing equipment, and non-renewable. In recent years, lignocellulosic fillers used to reinforce thermoplastics, especially polypropylene (PP), have expanded due to their strength, low density, relatively high aspect ratio and environmental benefits. Lignocellulosic materials such as wood fiber, wood flour, cellulose fiber, flax, and hemp have been given more attention by polymer manufactures (Bataille et al. 1989; Karnani et al. 1997). Futhermore, the micro/nanofibrils isolated from natural fibers have much higher mechanical properties as reported by Sakurada et al. (1962) that the cellulose crystal regions are a bundle of stretched cellulose chain molecules with Young`s modulus of 150 GPa and strength in the order of 10 GPa. Thus the micro/nanofibrils has the potential as the reinforcing materials to create innovative nanocomposites (Herrick et al. 1983; Stenstad et al. 2008; Turbak et al. 1983). Nevertheless, such fibers are used only to a limited extent in industrial practice, which may be explained by difficulties in achieving acceptable dispersion levels (Helbert 1996).

Two main methods, the chemical method, mainly by strong acid hydrolysis and mechanical method including a high intensity ultrasonication (Cheng, 2007a, 2007b; Wang & Cheng 2009), a high-pressure homogenizer treatment (Dufresne et al. 1997; Herrick et al. 1983; Nakagaito and Yano 2005; Stenstad et al. 2008; Turbak et al. 1983), a high pressure grinder treatment and a microfluidizer (Zimmermann et al. 2004), have been used to generate cellulose products. The product came from chemical method was described by cellulosic whisker or cellulose nanocrystal. However, the product isolated from mechanical method was defined by cellulose microfibril or microfibrillated cellulose.

Rice straw represents a potentially valuable source of fiber and has the potential to alleviate the shortage of wood fiber and petroleum resources. It is easy to obtain and its fiber is more

flexible than wood fiber, which can highly reduced wear of the processing machinery, together with its abundance and low price, giving it more utilization value. Therefore, it can be used as a direct substitute for wood composites, and also can be used to make plastics composites (Wu et al. 2009). The fibril and fibril aggregates were generated from rice straw pulp cellulose fiber by a high intensity ultrasonication (HIUS) treatment and were used to reinforce polypropylene (PP) by a novel compounding machine, a minilab extruder with a materials cycle system.

The objective of this work was to use rice straw pulp cellulose fiber to prepare environmental-friendly rice straw fibril and fibril aggregates (RSF) and evaluate the fibril and fibril aggregates as a novel reinforcing material to compound polypropylene (PP)/ RSF nanocomposite. The scanning electron microscopy (SEM), wide angle X-ray diffraction (WAXD), laser diameter instrument (LDI) were used to evaluate the characteristics of RSF. The RSF/PP nanocomposite was prepared by novel extrusion process. The interface compatibility and tensile properties of nanocomposite were investigated by FTIR and tensile test, respectively.

2. Materials and methods

The isotactic polypropylene (iPP) was supplied by FiberVisions, Georgia, in the form of homopolymer pellets with a melt flow index of 35g/10 min (230 ^{o}C, 160 g) and a density of 0.91 g cm^{-3}. The reinforcing filler was rice straw fibril and fibril aggregates (RSF) obtained from rice straw pulp fiber (Taonan paper and pulp company, Jilin province, North-east of China) that was cut to pass a screen (room temperature and relative humidity of 30%) with holes of 1 mm in diameter by a Willey mill before treatment. The maleated polypropylene (MAPP) was used as compatibilizing agent and Epolene G-3003 P has an acid number of 6 and a molecular mass of 125 722.

2.1 Fibril isolation

The milled rice straw pulp fiber was soaked in distilled water for more than 24 h, and then treated by high intensity ultrasonication (Sonics & Materials. INC, CT, 20kHz, Model 1500 W) for 30 min with 80% power level. After ultrasonication treatment, the obtained RSF aqua compound was kept in frozen.

2.2 Freeze drying

In order to avoid the aggregation of isolated RSF, the frozen RSF aqua compound was freeze-dry in Food Science, the University of Tennessee, Knoxville, TN, USA. The conditions of freeze drier (Virtis Genesis 12 EL) were -20 ^{o}C to + 20 ^{o}C over 4 days in 5 ^{o}C increments.

2.3 Compounding

The freeze-dry RSF was milled by a food processor and kept into a dessicator. The RSF/ PP nanocomposite was made by blending PP pellets with 1~6% MAPP (ratio of PP weight, wt%) and 2~11% RSF (ratio of total weight, wt%). All materials were then fed into a Haake Mini-Lab twin-screw extruder (Thermo Electron Corp., Hamburg, Germany). The blends were processed for 10 min, 20 min, 30 min at 50 rpm and 180 ^{o}C, 190 ^{o}C and 200 ^{o}C using a

counter-rotating screw configuration, respectively. The RSF/ PP nanocomposite was then extruded through a 2.5 mm cylindrical die. The extruder strands were granulated and hot pressing at a temperature of 175 °C and a pressure of 5 MPa for 10 min. The obtained sheets with nominal thickness of 270 μm were conditioned at 23 ± 2 °C and 50 ± 5% relative humidity for not less than 40 h prior to tensile test in accordance with Procedure A of Practice D 618.

Sample	PP	MAPP	RSF
PP	100	0	0
PP2M	98	2	0
PP2M2R	96	2	2
PP2M5R	93	2	5
PP2M8R	90	2	8
PP2M11R	87	2	11
PP1M	99	1	0
PP2M	98	2	0
PP3M	97	3	0
PP4M	96	4	0
PP5M	95	5	0
PP6M	94	6	0
PP1M5R	94	1	5
PP2M5R	93	2	5
PP3M5R	92	3	5
PP4M5R	91	4	5
PP5M5R	90	5	5
PP6M5R	89	6	5

Table 1. Proportion of RSF/PP nanocomposite (by weight, %)

2.4 Fibril diameter test

The laser diameter instrument (Winner 2005, Qingdao, China) was used to investigate the diameter distribution after HIUS treatment. The sample concentration for testing was 1.526% and three levels were tested for the sample.

2.5 Cellulose crystallinity

The wide angle X-ray diffraction (WAXD) was used to study the crystallinities of treated and untreated rice straw fiber and fibril aggregates. The Segal method was used to calculate the crystallinities of the samples (Cheng et al. 2007b; Thygesen et al. 2005). The equipment (Material Data. Inc. DX-2000) was a pinhole type camera that recorded the patterns on Fuji image plates. The operating voltage was 40 kV, current was 30 mA, and the exposed period was 3000s using CuKa radiation with a wavelength of 0.15418 nm. The crystallinity is

defined as the ratio of the amount of crystalline cellulose to the total amount of sample material including crystalline and amorphous parts. The Turley method was used to calculate the crystallinity (CrI) of the samples (Thygesen et al. 2005).

2.6 Mechanical characteristic

The tensile measurements were conducted on an Instron testing machine (Model 5567) with a length of 20 mm between the top and bottom clamps, a crosshead speed of 1 mm/min, and a load cell of 30 kN (Cheng et al. 2007a). The specimens were cut to drum shapes with width of 5 mm for the narrow portion and total length of 40 mm. Eight specimens were tested for each extruder condition according to the ASTM D 882 standard test method for tensile properties of thin plastic sheeting (ASTM D882-02). The overall significant differences of the influences on the tensile modulus and strength of polypropylene reinforced with RSF under different extruder conditions were conducted using a Statistic Analysis System (SAS) JMP version 6.0.2 software (SAS Institute, Cary, NC, USA).

2.7 FTIR testing

The functions of samples were tested by FTIR (Nicolet 380) accompanying with ATR. The sample scanning times was 64, the ratio of differentiate was 8.000, sampling plus was 2.0, the speed of moving lens was 0.6329, diaphragm was 100.00, wave range was 4000~400cm^{-1}.

2.8 Morphology characteristic

Polarized light microscopy (PLM, Olympus-BX51) and a digital image analysis software package (ImageJ) were used to observe the distributions of the RSF in the RSF/PP nanocomposite. The fractured surfaces of nanocomposite after tensile test were investigated by a scanning electron microscopy (SEM, LEO 1525). The freeze-dry samples were observed by SEM. The voltages were 5-10 kV and various magnification levels were used to obtain images.

3. Results and discussion

3.1 Morphology characteristic

Figure 1 was the distribution of RSF diameters treated by HIUS. As seen in the figure, the distribution of diameters of RSF ranged from 0.1 μm to 80 μm by HIUS treatment. The percentage was 6.3% of RSF which diameters were less than 500 nm; almost 90 percents of RSF distributed between 7.0 μm and 80 μm; the average diameter was 41 μm.

3.2 Crystallinity of fibers and fibrils

According to (Thygesen et al. 2005), the crystallinity of treated rice straw cellulose fiber was 72.9%, which was higher than untreated rice straw cellulose fiber of 71.3%. The reason may be that some of the amorphous cellulose were degraded and removed during the ultrasonication treatment. High crystalline fibers and fibril aggregates could be more effective in achieving higher reinforcement for composite materials (Eichhorn & Young 2001).

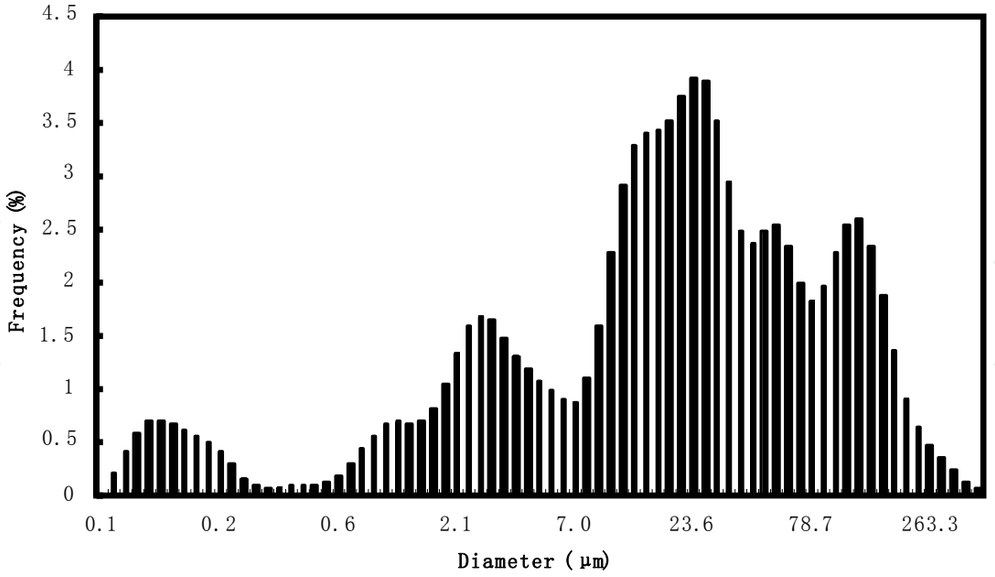

Fig. 1. Distribution of RSF diameters treated by HIUS

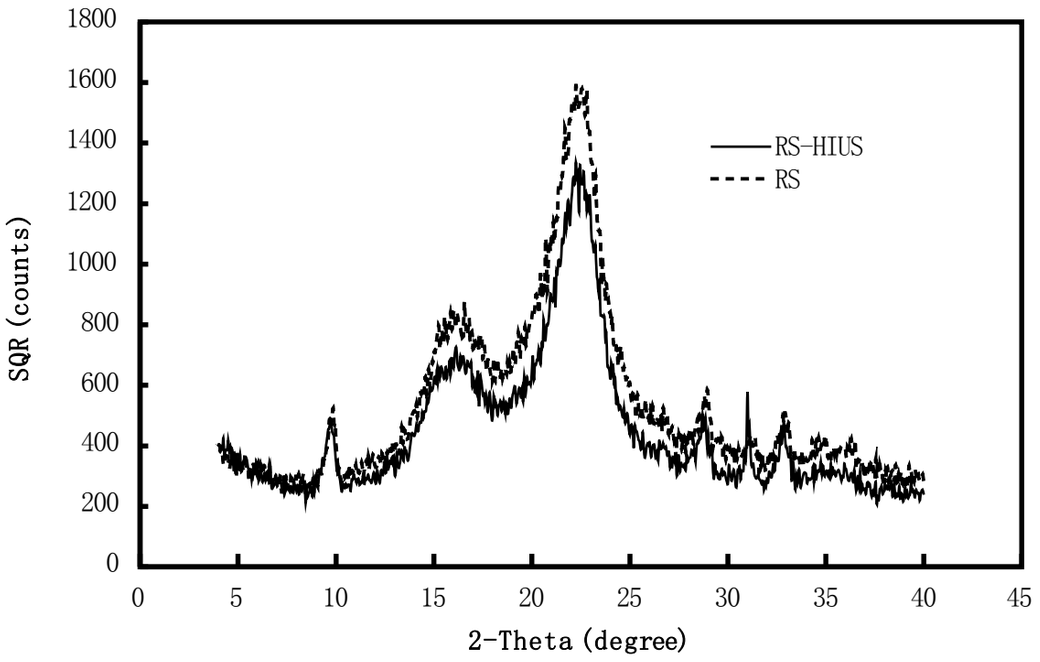

Fig. 2. CrI of untreated sample and sample treated by HPH

3.3 Effect of compounding conditions on RSF/PP nanocomposite tensile properties

The tensile strength of RSF/PP nanocomposite is shown in figure 3. The tensile strength of 5% rice straw fibril reinforcing PP nanocomposite was lower than PP/MAPP polymer. For the RSF/PP nanocomposite, the tensile strength increased with increasing cycle time from 10 min to 30 min at 180 °C. And the maximum value of tensile strength was 31.2 Mpa that appeared at the conditions of 190 °C, 20 min.

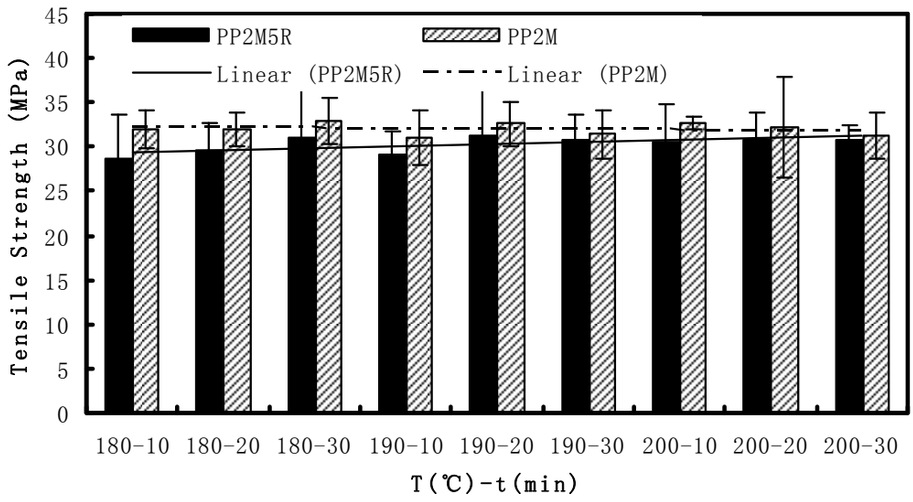

Fig. 3. Tensile strength of different extruder conditions

Figure 4 is the elastic modulus of PP/MAPP polymer and RSF/PP nanocomposite. The elastic modulus increased after added the 5% rice straw fibrils into the PP/MAPP polymer. For the PP/MAPP polymer, the elastic modulus increased significantly (R^2 = 0.53) with increasing compounding temperature and extruder cycle time. However, for the RSF/PP nanocomposite, the elastic modulus decreased with increasing compounding temperature and extruder cycle time, but this trend was not distinct.

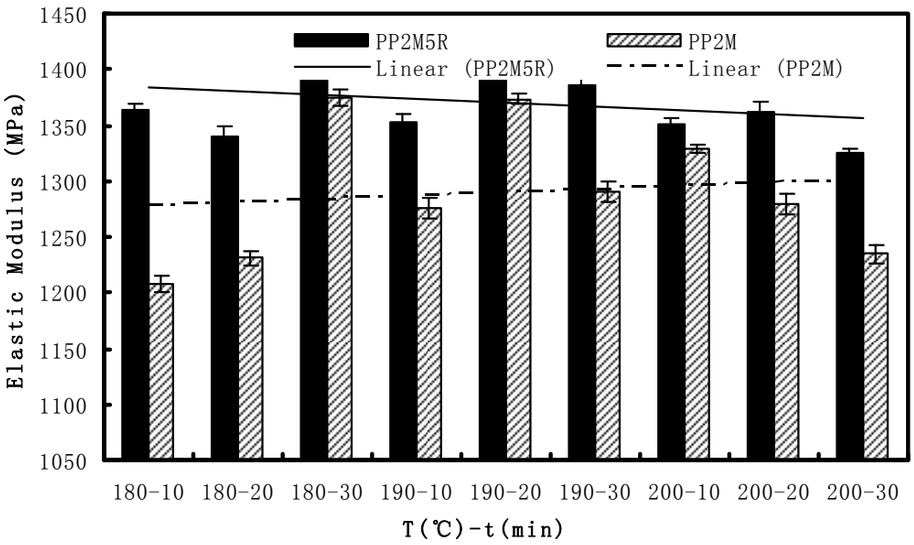

Fig. 4. Elastic modulus of different extruder conditions

The elongation at break was higher in PP/MAPP polymer than RSF/PP nanocomposite as shown in figure 5. With increasing compounding temperature and extruder cycle time the elongation at break decreased significantly (R^2=0.71) in PP/MAPP polymer, however, there had no big difference in RSF/PP nanocomposite.

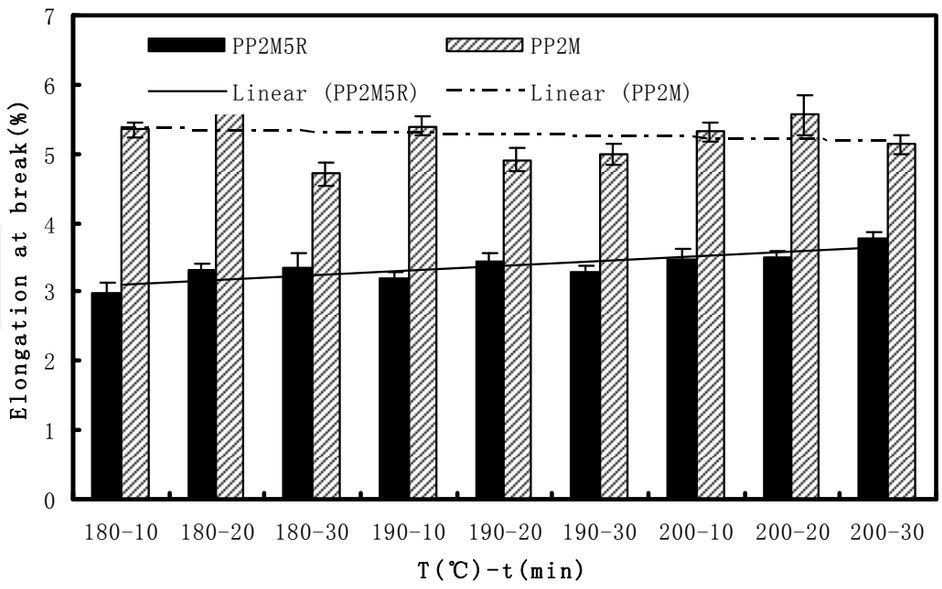

Fig. 5. Elongation of different extruder conditions

3.4 Effect of different RSF loadings on RSF/PP nanocomposite tensile properties

The tensile strength of RSF/PP nanocomposite with different fibril loadings is shown in figure 6. As the reference, the tensile strength of PP/MAPP polymer was also tested. The tensile strength at 5% RSF loading was up to the maximum value, 31.7 MPa, which was a little higher than the value of PP/MAPP polymer, 30.8 MPa. With increasing the fibril loadings the tensile strength decreased, but not distinct ($R^2 = 0.23$).

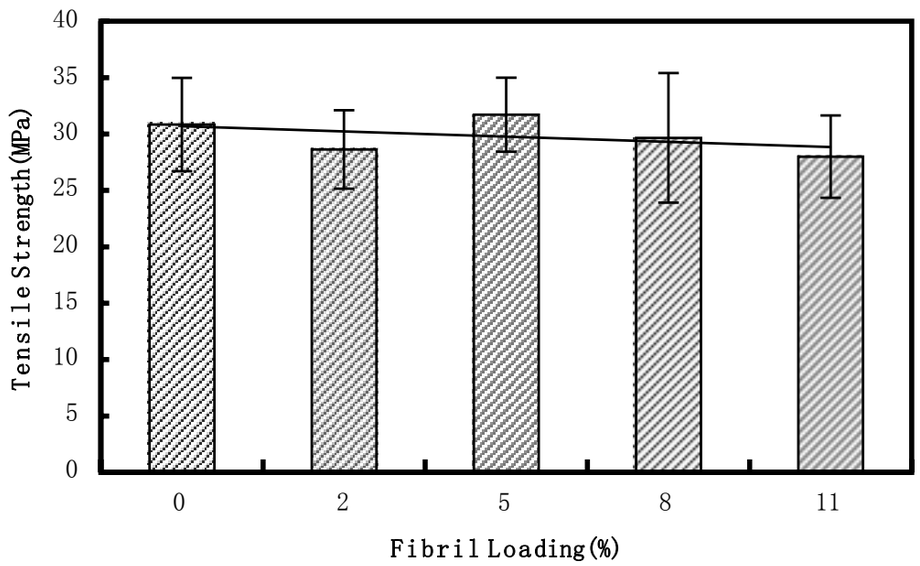

Fig. 6. Tensile strength of different fibril loadings

Figure 7 shows the elastic modulus of RSF/PP nanocomposite with different fibril loadings. The values were higher in RSF/PP nanocomposite than in PP/MAPP polymer. The fibril loadings from 2% to 8%, the elastic modulus increased significantly (R^2 = 0.70). The maximum was 1621 MPa at the 8% RSF, which was 17% higher than the value of PP/MAPP polymer. From 8% to 11% of RSF, the elastic modulus decreased.

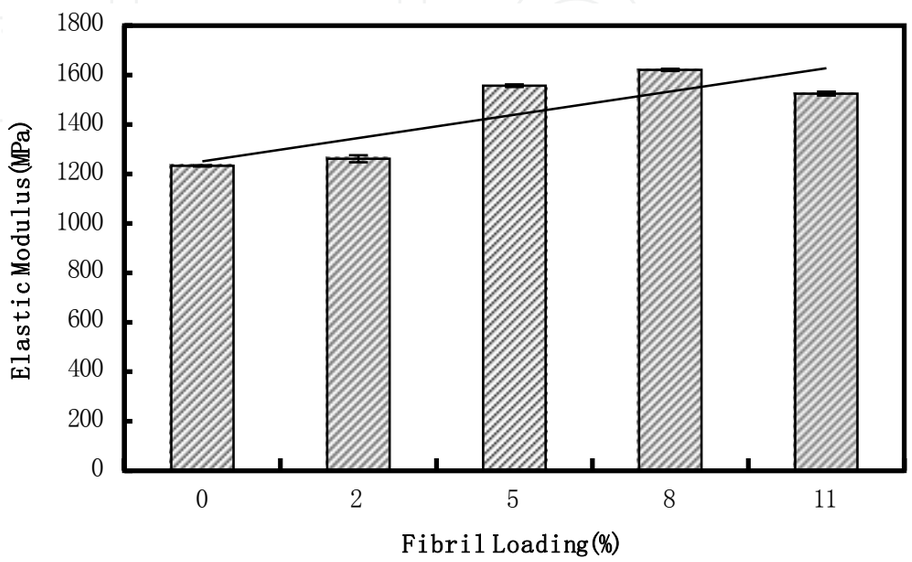

Fig. 7. Elastic modulus of different fibril loadings

The elongation at break showed a significant decreasing trend (R^2 = 0.89) with increasing the fibril loading (figure 8).

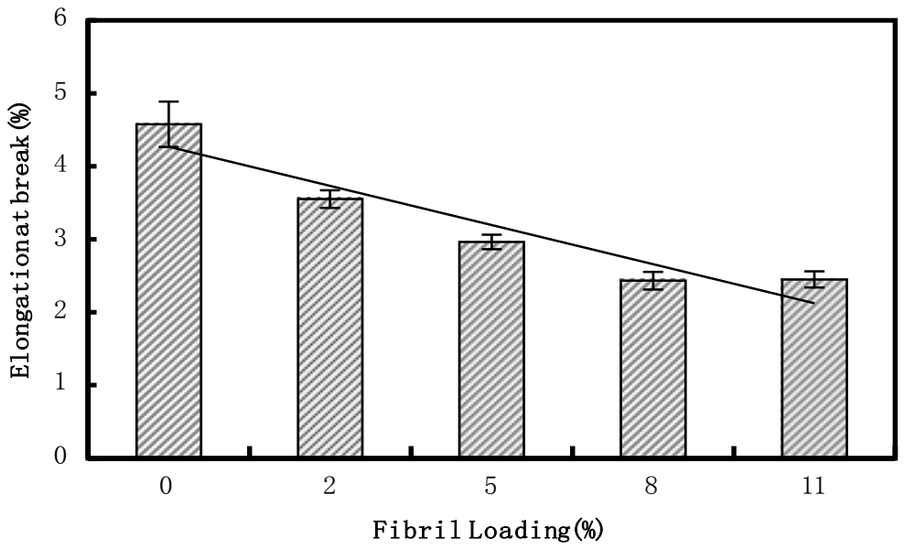

Fig. 8. Elongation of different fibril loadings

3.5 Effect of MAPP content on RSF/PP nanocomposite tensile properties

The tensile strength of PP/MAPP polymer decreased with increasing MAPP content from 1% to 6%, but not significant (figure 9). However, it showed a slightly increasing trend in RSF/PP nanocomposite as the MAPP content from 2% to 5%, then decreased when MAPP up to 6%.

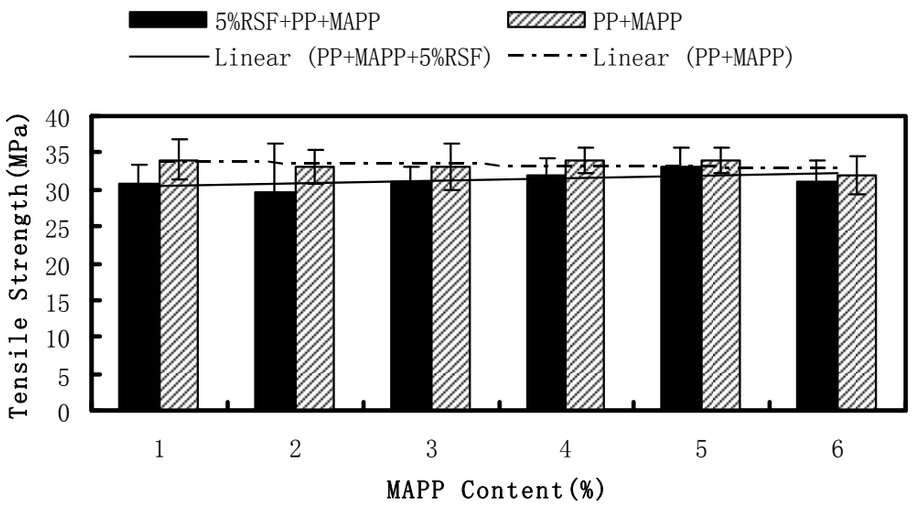

Fig. 9. Tensile strength of different MAPP contents

The elastic modulus and elongation at break appeared decreasing trend with increasing MAPP content both in PP/MAPP polymer and RSF/PP nanocomposite, as shown in figures 10 and 11. But the trends were not distinct according to the linear analysis.

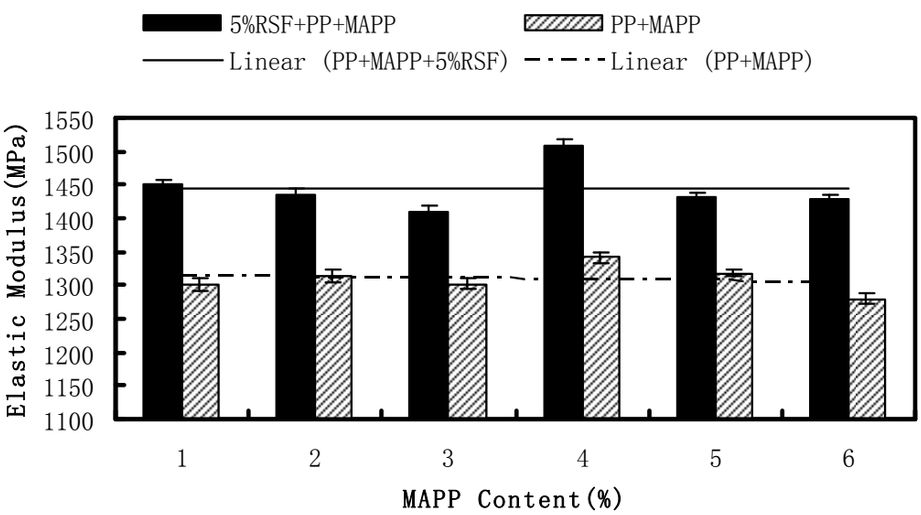

Fig. 10. Elastic modulus of different MAPP contents

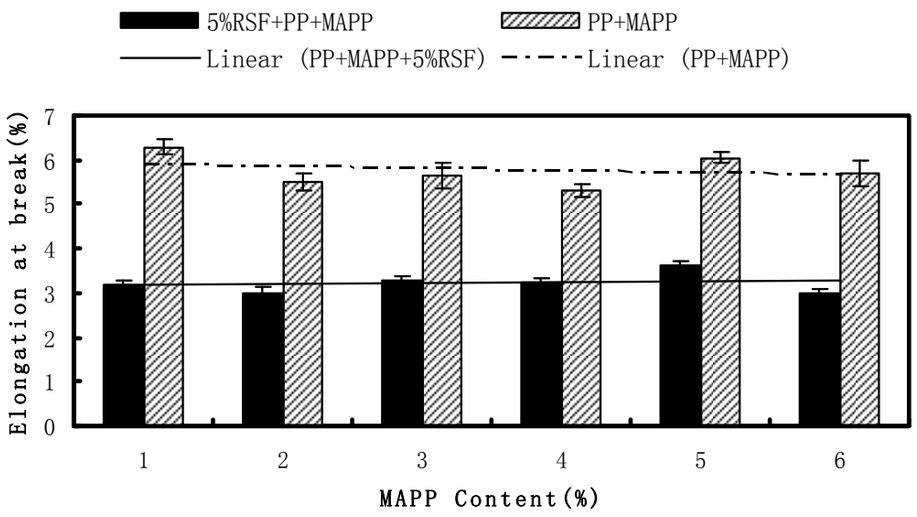

Fig. 11. Elongation at break of different MAPP contents

3.6 Effect of different ultrasonication treat condition on tensile properties

Figure 12 is the tensile strength of RSF/PP nanocomposite with different ultrasonication treat time RSF as the filler. For the ultrasonication treatment, the rice straw cellulose fiber content was 0.5% and 1%, respectively. As seen in this figure, the tensile strength increased distinctly (R^2=0.70 and R^2=0.96) with increasing ultrasonication treat time. The tensile strength of 0.5% rice straw cellulose fiber content was lower than 1% rice straw cellulose fiber content at different ultrasonication treat time.

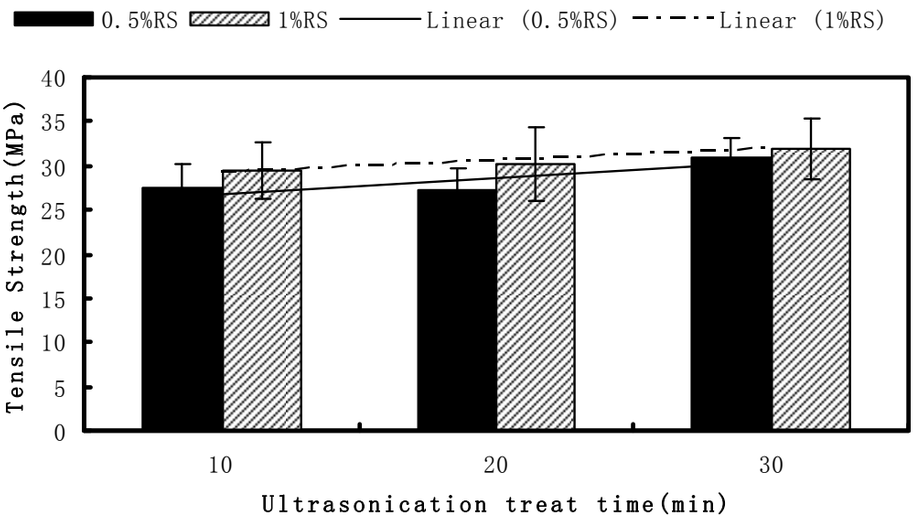

Fig. 12. Tensile strength of different ultrasonication treat time

The elastic modulus and elongation at break increased with increasing ultrasonication treat time as shown in figures 13 and 14. And also the elastic modulus and elongation at break were higher with 1% rice straw cellulose fiber content treated by ultrasonication as filler than 0.5%.

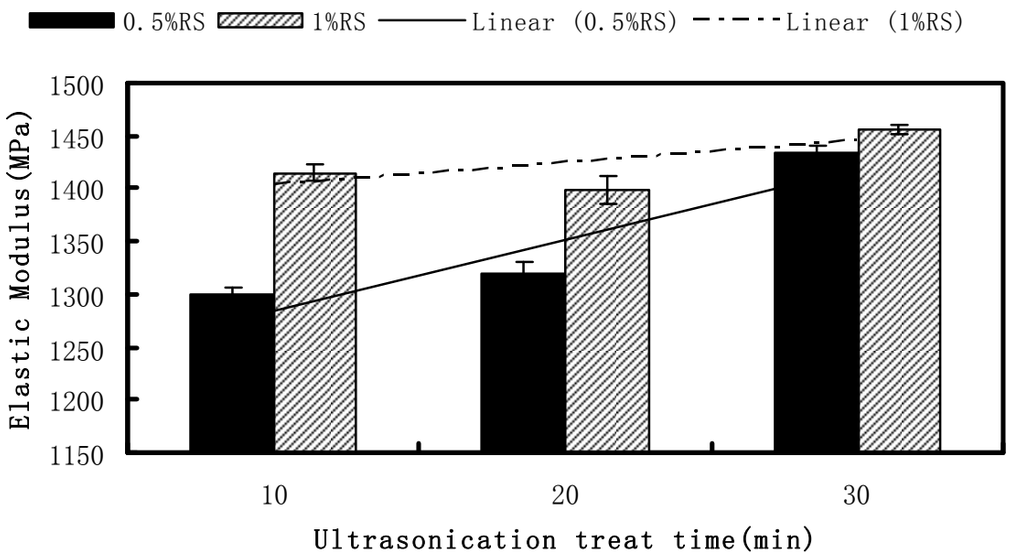

Fig. 13. Elastic modulus of different ultrasonication treat time

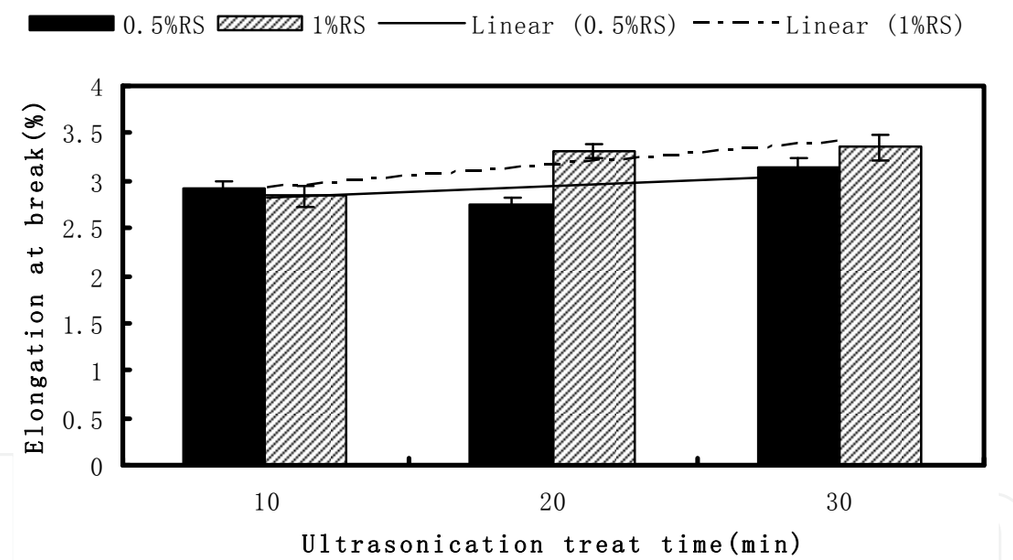

Fig. 14. Elongation at break of different ultrasonication treat time

3.7 FTIR analysis of RSF/PP nanocomposite

Figure 15 showed the FTIR spectra of PP, RSF/PP, RSF from up to down.

When adding MAPP and RSF into PP matrix, the FTIR spectra showed prodigious changes. CH_3 deformation of asymmetry stretching and CH_2 symmetry stretching moved to higher wavenumbers. Moreover, the frequency of CH_3 symmetry deformation decreased (1374CM^{-1} to 1372 CM^{-1}). The existence of C-O-C stretching at 1224 CM^{-1}, 1074 CM^{-1} and 1028 CM^{-1} indicated that PP and RSF were consistent by adding MAPP. Table 2 listed the vibration peaks and assignments of peaks of RSF/PP nanocomposite.

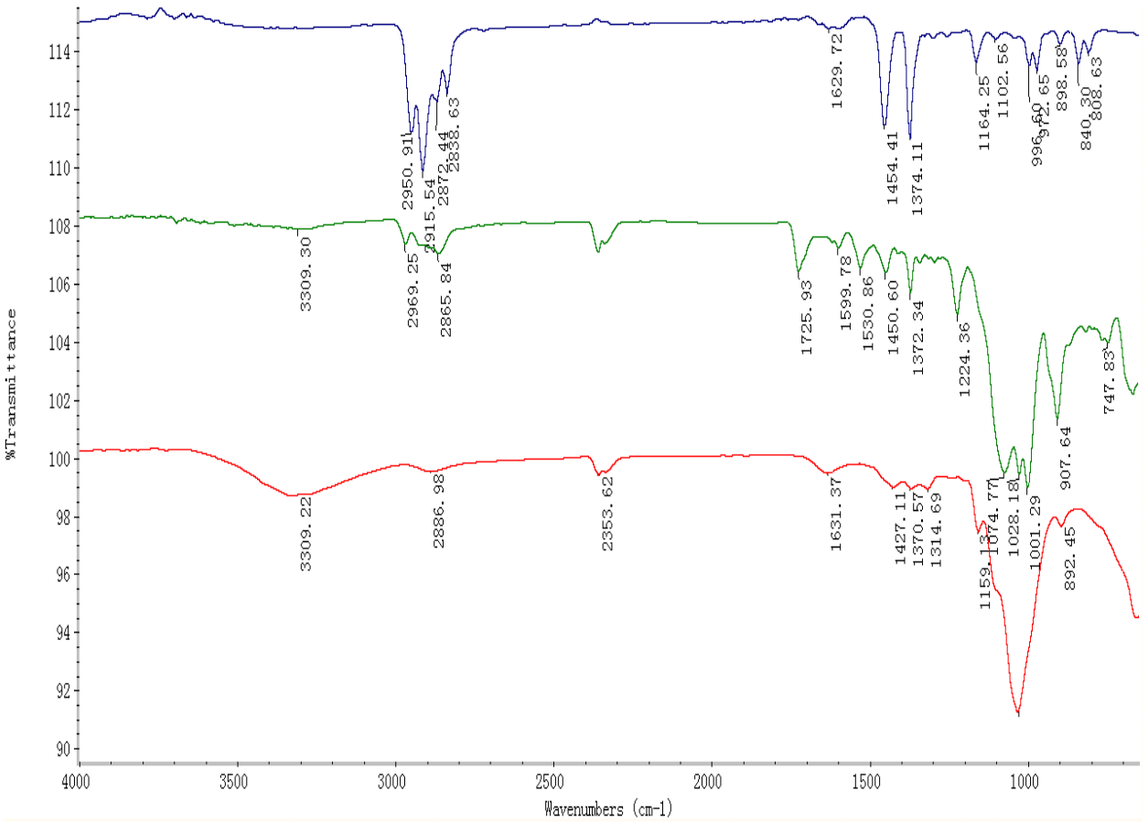

Fig. 15. FTIR curves of PP, RSF/PP nanocomposite and RSF

Wavenumber (cm-1)	Assignments
3309	-OH stretching
2969	CH3 deformation of asymmetry stretching
2865	CH2 symmetry stretching
1725	C=O stretching
1450	CH3 asymmetry deformation
1450	CH2 shearing
1372	CH3 symmetry deformation
1224, 1074, 1028	C-O-C stretching

Table 2. FTIR vibration peaks and assignments of peaks of RSF/PP nanocomposite

3.8 Morphology characteristics of fibers and fibrils

After ultrasonication treatment, the rice straw cellulose fiber changed into small size fibrils. The SEM pictures showed the appearance of untreated (figure 16a) and treated (figure 16b) rice straw cellulose fiber.

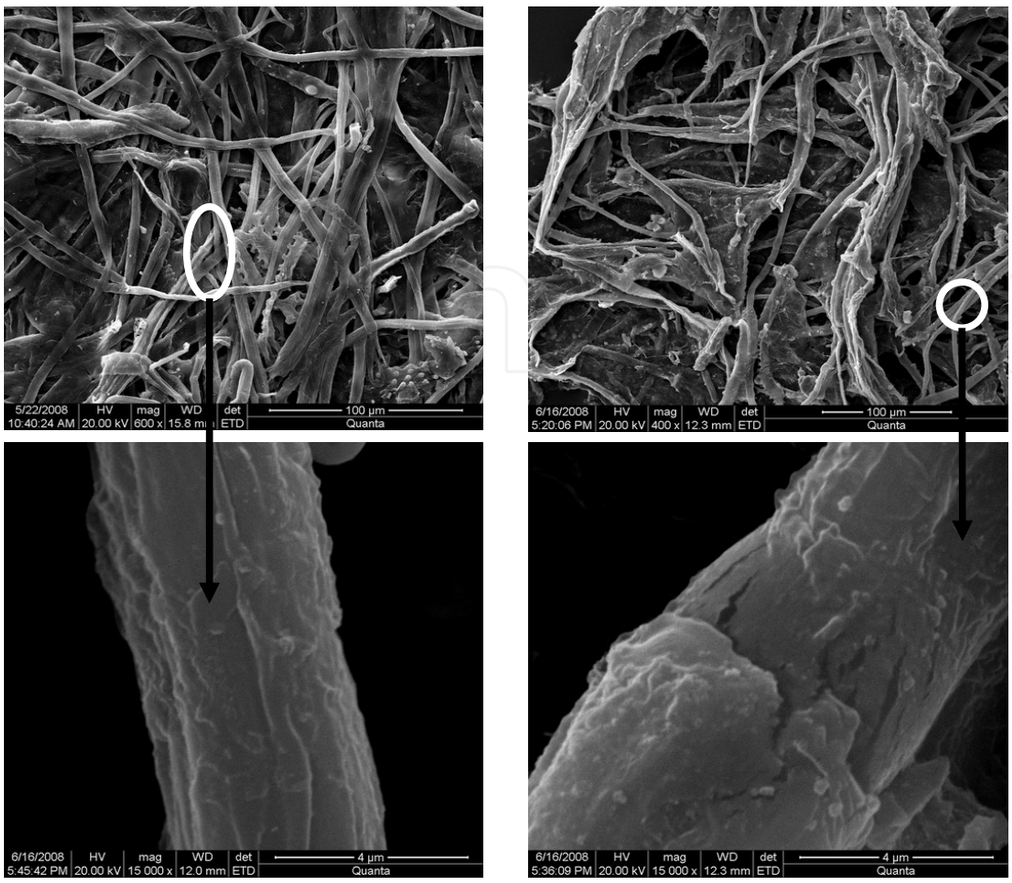

Fig. 16. SEM photos of untreated sample (a, left) and treated sample (b, right)

It can be seen from figure 13b inset figure that the fibrils peeled off from the fibers and the ultrasonication treatment made the surface of fibers producing fractures. The fibrils and microfibrils can form a kind of micro/nano-order-unit web-like network structure (Nakagaito & Yano, 2005), which can greatly expanded in the surface area that characteristic the RSF and increase the compounding abilities between fibrils/mircrofibrils and polymer. After the ultrasonication treatment, fibrils, fibrils aggregates and cellulose fibers together existed, and also the fibrils had a widely width (or diameter) ranges from tens of nanometer to micrometers as shown in figure 1. The fibrils with diameter less than 500 nm were peeled from the fibers, however, the fibril aggregates with diameter around 25 µm took the most place.

3.9 Fracture cross section morphology of RSF/PP nanocomposite

The fracture cross section morphology of RSF/PP nanocomposite after tensile test was observed by scanning electron microscopy (SEM). As shown in figure 17(a), the rice straw fibrils embedded into the polymer and exhibited better interaction with polymer. The fibrils were interconnected with the polymer and didn`t pull out from the polymer during the tensile test. However, the bigger size fiber still can be seen in the nanocomposite and it appeared the gas between the fiber and the polymer (figure 17b), which proved that the bigger size cellulose fiber and the polymer can not bond together easily or the compatibility was not as good as the fibril filler. And this may be the reason that the tensile strength in RSF/PP nanocomposite was

lower than PP/MAPP polymer. To improve the degree and homogenization of fibril will be a good way to increase the compatibility between RSF and polymer.

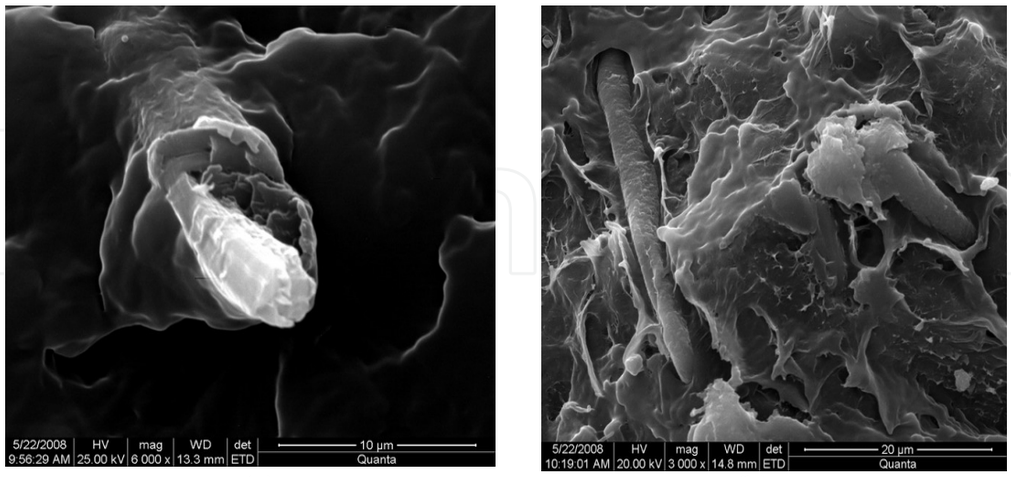

(a) (b)

Fig. 17. Fracture cross section SEM photos of RSF/PP nanocomposite after tensile test

It was seen in figure 18 of PLM picture, the distribution of RSF in the RSF/PP nanocomposite was good, which indicated the minilab extruder with a cycle system was a suitable machine to compound the polymer and cellulose fibrils.

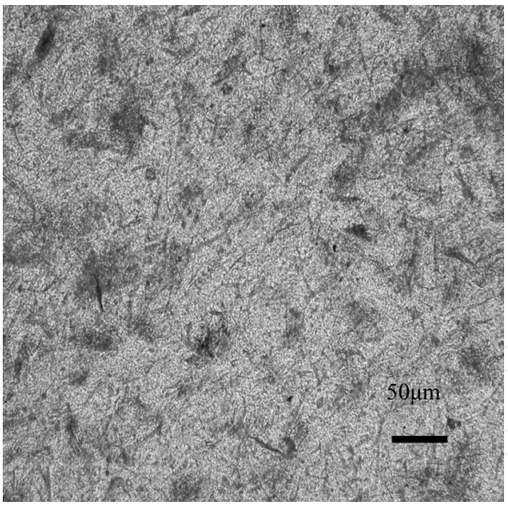

Fig. 18. PLM photo of RSF distribution in RSF/PP nanocomposite

4. Conclusions

The distribution of diameters of RSF ranged from 0.1 µm to 80 µm by HIUS treatment. The percentage was 6.3% of RSF which diameters were less than 500 nm; almost 90 percents of RSF distributed between 7.0 µm and 80 µm; the average diameter was 41 µm. The relative crystallinities of untreated rice straw cellulose fibers and rice straw cellulose fibers treated by HIUS were 71.3% and 72.9%, respectively.

The elastic modulus increased of RSF/PP nanocomposite comparing with PP/MAPP polymer. However, the tensile strength and elongation at break of 5% rice straw fibril reinforcing PP nanocomposite was lower than PP/MAPP polymer at different extruder compounding conditions. The tensile strength at 5% RSF loading was up to the maximum value, 31.7 MPa, which was a little higher than the value of PP/MAPP polymer, 30.8 MPa. The maximum was 1621 MPa at the 8% RSF, which was 17% higher than the value of PP/MAPP polymer. The elongation at break showed a significant decreasing trend with increasing the fibril loading. There was no distinct influence of tensile strength and elongation of nanocomposite and PP/MAPP polymer with increasing MAPP content. The maximum of elastic modulus was 1509 MPa at the 4% of MAPP. The tensile properties increased distinctly with increasing ultrasonication treat time. The tensile strength of 0.5% rice straw cellulose fiber content was lower than 1% rice straw cellulose fiber content at different ultrasonication treat time.

After adding MAPP and RSF into PP matrix, the FTIR spectra had big changes. The absorption peak of ester bonds (C-O-C) appeared at 1224 CM-1, 1074 CM-1 and 1028 CM-1, which proved that there had been a good compatibility between PP matrix and RSF. The SEM images showed: the fibrils were embedded into the PP/MAPP matrix, during the tensile test, which were not pulled out from the matrix.

5. Acknowledgment

The work is supported by Natural Science Foundation of China (31100417) and (31070492).

6. References

ASTM D (D 882 - 02) Standard test method for tensile properties of thin plastic sheeting.

Bataille, P.; Ricard, L. & Sapieha, S. (1989). Effects of cellulose fibers in polypropylene composites. *Polymer Composites*, Vol. 10, pp. 103, ISSN 1548-0569

Cheng, Q.; Wang, S.; Rials, T. & Lee, S. (2007a). Physical and mechanical properties of polyvinyl alcohol and polypropylene composite materials reinforced with fibril aggregates isolated from regenerated cellulose fibers. *Cellulose*, Vol. 14, pp. 593-602, ISSN 0969-0239

Cheng, Q.; Wang, S.; Zhou, D.; Zhang, Y. & Rials, T. (2007b). Lyocell-derived cellulose fibril and its biodegradable nanocomposite. *Journal of Nanjing Forestry University*, Vol. 31, No. 4, pp. 21-26, ISSN 1000-2006

Dufresne, A.; Cavaille, J.Y. & Vignon, M.R. (1997). Mechanical behavior of sheets prepared from sugar beet cellulose microfibrils. *Journal of Applied Polymer Science*, Vol. 64, No. 6, pp. 633-639, ISSN 1097-4628

Eichhorn, S.J. & Young, R.J. (2001). The Young`s modulus of a microcrystalline cellulose. *Cellulose,* Vol. 8, No. 3, pp. 197-207, ISSN 0969-0239

Herrick, F.W.; Casebier, R.L.; Hamilton, J.K. & Sandberg, K.R. (1983). Microfibrillated cellulose: morphology and accessibility. *Journal of Applied Polymer Science*, Vol. 37, pp. 797-813, ISSN 1097-4628

Helbert, W. J.; Cavaillé, Y.; Dufresne, A. (1996). Thermoplastic nanocomposites filled with wheat straw cellulose whiskers. Part I: processing and mechanical behavior. *Polymer Composites,* Vol. 17, pp. 604-611, ISSN 1548-0569

Karnani, R.; Mohan, K. & Ramini, N. (1997). Biofiber-reinforced polypropylene composites. *Polymer Engineering & Science*, Vol. 37, pp. 476, ISSN 1548-2634

Nakagaito, A.N. & Yano, H. (2005). Novel high-strength biocomposites based on micriofibrillated cellulose having nano-order-unit web-like network structure. Journal of Applied Physics, Vol. 80, pp. 155-159, ISSN 0021-8979

Sakurada, I.; Nukushina, Y. & Ito, T. (1962). Experimental determination of elastic modulus of crystalline regions in oriented polymer. *Journal of Polymer Science Part B: Polymer Physics*, Vol, 57, No. 165, pp. 651-660, ISSN 1099-0488

Stenstad, P.; Andresen, M. & Tanem, B. (2008). Chemical surface modifications of microfibrillated cellulose. *Cellulose*, Vol. 15, pp. 35-45, ISSN 0969-0239

Thygesen, A.; Oddershede, J.; Lilholt, H.; Thosmsen, A.B. & Stahl, K. (2005). On the determination of crystallinity and cellulose content in plant fibres. *Cellulose*, Vol. 12, No. 6, pp. 563-576, ISSN 0969-0239

Turbak, A.F.; Snyder, F.W. & Sandberg, K.R. (1983). Microfibrilated cellulose, a new cellulos product: properties, uses, and commercial potential. *Journal of Applied Polymer Science*, Vol. 37, pp. 815-827, ISSN 1097-4628

Wang, S. & Cheng, Q. (2009). A novel method to isolate fibrils from cellulose fibers by high intensity ultrasonication. Part I. Process optimization. *Journal of Applied Polymer Science*, Vol. 113, pp. 1270-1275, ISSN 1097-4628

Wu, Y.; Zhou, D.G.; Wang, S.Q.; Zhang, Y. (2009) Polypropylene composites reinforced with rice straw micro/nano fibrils isolated by high intensity ultrasonication. *BioResources*, Vol. 4, pp. 1487-1497, ISSN 1930-2126

Zimmermann, T.; Pohler, E. & Geiger, T. (2004). Cellulose fibrils for polymer reinforcement. *Advanced Engineering Materials,* Vol. 6, No. 9, pp. 754-761, ISSN 1527-2648

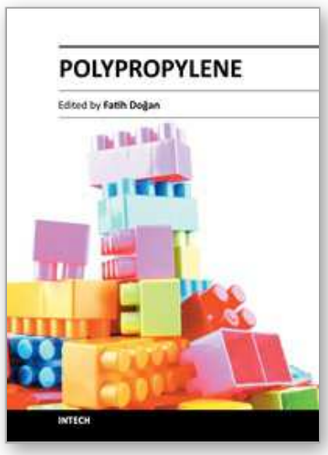

Polypropylene

Edited by Dr. Fatih Dogan

ISBN 978-953-51-0636-4
Hard cover, 500 pages
Publisher InTech
Published online 30, May, 2012
Published in print edition May, 2012

This book aims to bring together researchers and their papers on polypropylene, and to describe and illustrate the developmental stages polypropylene has gone through over the last 70 years. Besides, one can find papers not only on every application and practice of polypropylene but also on the latest polypropylene technologies. It is also intended in this compilation to present information on polypropylene in a medium readily accessible for any reader.

How to reference

In order to correctly reference this scholarly work, feel free to copy and paste the following:

Yan Wu, Dingguo Zhou, Siqun Wang, Yang Zhang and Zhihui Wu (2012). Polypropylene Nanocomposite Reinforced with Rice Straw Fibril and Fibril Aggregates, Polypropylene, Dr. Fatih Dogan (Ed.), ISBN: 978-953-51-0636-4, InTech, Available from: http://www.intechopen.com/books/polypropylene/polypropylene-nanocomposite-reinforced-with-rice-straw-fibril-and-fibril-aggregates

INTECH
open science | open minds

InTech Europe
University Campus STeP Ri
Slavka Krautzeka 83/A
51000 Rijeka, Croatia
Phone: +385 (51) 770 447
Fax: +385 (51) 686 166
www.intechopen.com

InTech China
Unit 405, Office Block, Hotel Equatorial Shanghai
No.65, Yan An Road (West), Shanghai, 200040, China
中国上海市延安西路65号上海国际贵都大饭店办公楼405单元
Phone: +86-21-62489820
Fax: +86-21-62489821

IntechOpen